Prediction of the Unsteady Behavior of Maneuvering Aircraft by CFD Aerodynamic, Flight-Mechanic and Aeroelastic Coupling

Andreas Schütte, Gunnar Einarsson, Axel Raichle, Britta Schöning
Deutsches Zentrum für Luft- und Raumfahrt e.V. in der Helmholtz-Gemeinschaft,
German Aerospace Center, Member of the Helmholtz Association
Institute of Aerodynamics and Flow Technology,
Lilienthalplatz 7, D-38108 Braunschweig

Andreas.Schuette@dlr.de, Gunnar.Einarsson@dlr.de, Axel.Raichle@dlr.de, Britta.Schoening@dlr.de

Wulf Mönnich
Deutsches Zentrum für Luft- und Raumfahrt e.V. in der Helmholtz-Gemeinschaft,
Institute of Flight Systems,
Lilienthalplatz 7, D-38108 Braunschweig

Wulf.Moennich@dlr.de

Jens Neumann, Jürgen Arnold
Deutsches Zentrum für Luft- und Raumfahrt e.V. in der Helmholtz-Gemeinschaft,
Institute of Aeroelastics,
Bunsenstrasse 10, D-37073 Göttingen

Jens.Neumann@dlr.de, Juergen.Arnold@dlr.de

Thomas Alrutz
Deutsches Zentrum für Luft- und Raumfahrt e.V. in der Helmholtz-Gemeinschaft,
Institute of Aerodynamics and Flow Technology,
Bunsenstrasse 10, D-37073 Göttingen

Thomas.Alrutz@dlr.de

Jörg Heinecke, Tomas Forkert, Holger Schumann
Deutsches Zentrum für Luft- und Raumfahrt e.V. in der Helmholtz-Gemeinschaft,
Simulation and Software Technology,
Linder Höhe, D-51147 Köln

Joerg.Heinecke@dlr.de, Tomas.Forkert@dlr.de, Holger.Schumann@dlr.de

ABSTRACT

An overview about recent results of the DLR-Project SikMa-"Simulation of Complex Maneuvers" is presented. The objective of the SikMa-Project is to develop a numerical tool to simulate the unsteady aerodynamics of a free flying aeroelastic combat aircraft, by use of coupled aerodynamic, flight-mechanic and aeroelastic computations. To achieve this objective, the unstructured, time-accurate flow-solver TAU is coupled with a computational module solving the flight-mechanic equations of motion and a structural mechanics code determining the structural deformations. By use of an overlapping grid technique (chimera), simulations of a complex configuration with movable control-surfaces are possible.

NATO/PFP UNCLASSIFIED

**Prediction of the Unsteady Behavior of Maneuvering Aircraft by
CFD Aerodynamic, Flight-Mechanic and Aeroelastic Coupling**

1. INTRODUCTION

The improvement of maneuverability and agility is a substantial requirement of modern fighter aircraft. Currently, roll-rates of 200°/s and more can be achieved, especially if the design of the aircraft is inherently unstable. Most of today's and probably future manned or unmanned fighter aircraft will be delta wing configurations. Already at medium angles of attack the flow field of such configurations is dominated by vortices developed by flow separation at the wings and the fuselage. The delay in time of vortex position and condition to the on-flow conditions of the maneuvering aircraft can lead to significant phase shifts in the distribution of loads. In such a case, reliable results for the analysis of the flight properties can only be achieved by a combined non-linear integration of the unsteady aerodynamics, the actual flight motion, and the elastic deformation of the aircraft structure.

Today, these types of data can only be obtained by flight tests, and not during the design period. Flight-tests, as well as modifications after the design phase, lead normally to an increase in costs. In order to decrease the costs incurred by extensive flight-tests and the post-design phase modifications, it would be helpful to have a tool which enables aircraft designers to analyze and evaluate the dynamic behavior during the design phase.

The main objective of this paper is to focus on the necessity for developing an interactive, multidisciplinary engineering tool for predicting the unsteady critical states of complex maneuvering aircraft. Such a simulation environment has to bring together aerodynamics, aeroelasticity and flight mechanics in a time-accurate simulation tool. In order to deliver such a tool in the near future, the DLR Project SikMa-"Simulation of Complex Maneuvers" has been initiated to combine these three disciplines into one simulation environment [18][19].

For validating the numerical simulations several wind tunnel experiments in both the low speed and transonic flow regime are be done within the SikMa project.

2. NOTATIONS

t	Time	l_μ	Aerodynamic mean chord
F	Reference area	V_∞	Free stream velocity
l_i	Chord length of the model	f	Frequency
Ma	Mach number	dy	Deformation increment in y-direction
Re	Reynolds number $[= V_\infty \cdot l_i / \nu]$	dz	Deformation increment in z-direction
c_p	Pressure coefficient $[= (p - p_\infty)/q_\infty]$		
q_∞	Dynamic pressure $[= \rho_\infty/2 \cdot V_\infty^2]$		
ω^*	Reduced frequency $[= 2\pi f \cdot l_i /V_\infty]$	Θ	Incidence angle, pitch at $\Phi=0°$
c_L	Lift coefficient $[= L/(q_\infty F)]$	Φ	Roll angle
c_M	Pitching moment coefficient $[= M/(q_\infty F l_i)]$	Φ_0	Initial roll angle
c_l	Rolling moment coefficient $[= L/(q_\infty F l_i)]$	η	Flap deflection angle
		α	Angle-of-attack
		$\Delta\alpha$	Angle-of-attack amplitude

NATO/PFP UNCLASSIFIED

**Prediction of the Unsteady Behavior of Maneuvering Aircraft by
CFD Aerodynamic, Flight-Mechanic and Aeroelastic Coupling**

3. NUMERICAL APPROACH

3.1 CFD Solver TAU

The behavior of the fluid-flow affecting the object of interest is simulated with the TAU-Code, a CFD tool developed by the DLR Institute of Aerodynamics and Flow Technology [9][10]. The TAU-Code solves the compressible, three-dimensional, time-accurate Reynolds-Averaged Navier-Stokes equations using a finite volume formulation. The TAU-Code is based on a hybrid unstructured-grid approach, which makes use of the advantages that prismatic grids offer in the resolution of viscous shear layers near walls, and the flexibility in grid generation offered by unstructured grids. The grids used for simulations in this paper were created with the hybrid grid generator Centaur, developed by Centaur Soft [3]. A dual-grid approach is used in order to make the flow solver independent from the cell types used in the initial grid. The unstructured grid approach is chosen due to its flexibility in creating grids for complex configurations, e.g. a full-configured fighter aircraft with control surfaces and armament, the capability of grid adaptation and straight forward parallelization of all the main TAU modules.

The TAU-Code consists of several different modules, among which are:

- The Pre-processor module, which uses the information from the initial grid to create a dual-grid and the coarser grids for multi-grid.

- The Solver module, which performs the flow calculations on the dual-grid.

- The Adaptation module, which refines and de-refines the grid in order to capture flow phenomena like vortex structures and shear layers near viscous boundaries, among others.

- The Deformation module, which propagates the deformation of surface-coordinates to the surrounding grid.

- The Post-processing module, which is used to convert TAU-Code result-files to formats usable by popular visualization tools.

The Solver module contains several upwind schemes, as well as a central scheme with artificial dissipation, which are available for the spatial discretization. For simulations of turbulent flows, the one-equation Spalart-Allmaras and several two-equation turbulence models are implemented. For steady computations either an explicit Runge-Kutta type time-stepping or an implicit LU-SSOR-scheme [5] are used in combination with the multi-grid technique. For time-accurate simulations an implicit dual-time stepping approach is used.

The TAU-Code can handle simulations containing multiple bodies in relative motion with one another, e.g motion of control surfaces with respect to the aircraft, by use of a hierarchical motion-node structure. The motion of each body can either be calculated internally by the TAU-Code, or supplied by an external program through a Python implemented external interface.

3.1.1 TAU-Code Module: Deformation

The Deformation module accepts deformed surface-coordinates either as absolute positions, or as relative displacements from the previous surface grid. User defined, rigid body motions of the surface coordinates can also be used to specify the grid deformation. The input used for the cases presented in this paper is a deformed surface-grid created by an external program. A deformed surface-grid, containing points with new absolute positions, is written to a file which the Deformation module reads. The deformation of the surface grid is propagated through the primary grid, and a new primary grid is created. The Preprocessor

NATO/PFP UNCLASSIFIED

**Prediction of the Unsteady Behavior of Maneuvering Aircraft by
CFD Aerodynamic, Flight-Mechanic and Aeroelastic Coupling**

module uses this new primary grid to create the dual fine and coarse grids required by the Solver module.

3.1.2 TAU-Code Module: Motion

The Motion module is not a stand-alone executable but a library of functions that handle the rigid-body translational and rotational transformation matrix calculations for the TAU-Code. The module is built to take advantage of naturally occurring hierarchical motion structures, where for example flaps and slats inherit the motion of the wing to which they are attached. Several modes of motion description are allowed, of which the most common are the following:

- periodic - which allows the user to enter a reduced frequency (usually obtained from experimental data), and describe the motion using a combination of Fourier and polynomial series. For periodic motions the user has to specify the number of time-steps per period, such that the Motion module can calculate the maximum time-step allowed, based on the specified reduced frequency.

- rigid - which allows the user to specify a physical time-step size while using the same type of motion description as for the periodic motion. For periodic motions the user has to calculate the appropriate time-step based on the desired number of time-steps per period. For non-periodic motions the user can select a time-step which can sufficiently resolve the prescribed motion.

- rotate - which allows the user to specify a constant rotation around a given axis using a reduced frequency as input parameter. The user has to specify the number of time-steps per period, such that the Motion module can calculate the maximum time-step allowed, based on the specified reduced frequency.

- external - which allows the user to create motion parameters (angles, rates, translation, displacement) in an external program and send those to the TAU-Code through a Python interface to the Motion module.

The rotation of a body can be described around either the body-fixed coordinate axis (as defined by the DIN 9300 standard), or around a vector defined in space (a so-called hinge-line vector). The translation of a body is specified in the body-fixed reference frame of the parent-node in the motion hierarchy (the inertial reference frame being the parent-node for the entire simulation); an exception to this is when the translation is obtained from the flight-dynamics interface, in that case the translation is specified in the body-fixed frame of the current node itself.

The Motion module uses the given input to create the transformation matrices required to determine the current position of the surface-grids relative to the inertial system, and the relative position of one grid with respect to another for multi-body simulations.

3.1.3 TAU-Code Extension: Chimera Technique

The chimera technique provides the capability to perform calculations with systems of overlapping grids. By allowing large relative body movement without the need for local remeshing or grid deformation, the technique is invaluable for the simulation of maneuvering combat aircraft, where large-amplitude control surface deflections and/or store release are a standard part of the simulation. The current implementation can handle multi-body simulations where the overlapping grid boundaries have been predefined; a version that allows 'automatic-hole-cutting' is currently under development. The chimera search algorithm, which is based on a state-of-the-art alternating digital tree (ADT), is available for both sequential and massively parallel architectures. A more detailed description of the chimera approach is given in [13].

3.2 Flight Mechanics

For the numerical simulation of the flight mechanics, the simulation environment SIMULA developed at the DLR Institute of Flight Systems is used [14]. SIMULA provides the three basic functionalities necessary for flight simulation and flight control purposes: trimming, i.e. the determination of the initial state and control values, linearization and stability analysis, and simulation, i.e. the numerical integration of the equations of motion.

Single and multi-body flight-mechanic models, ranging from 1 to 6 degrees of freedom, are made available to the simulation by SIMULA. The amount of data that is exchanged between SIMULA and TAU is of a scale that can be easily communicated directly through a TCP/IP socket connection, which is offered by the simulation environment TENT.

3.3 Structural Dynamics

For the coupling of the aerodynamic and structural dynamic simulations in the time domain, two different and independent approaches have been implemented to gain simulation redundancy and to minimize the project risk. Furthermore, it is necessary to have different approaches with adjusted structural dynamic models depending on the complexity of the simulation problem. Both approaches are based on a loose coupling scheme and use different software for the spatial coupling, structural dynamics and flight mechanics simulation. For the presented applications the loose coupling scheme is sufficient. The time increments on the CFD side are small enough so that the data exchange in each pseudo time step is not necessary. The quality of the coupling is considered by equilibrium verification of loads, energies and work at each physical time step.

For the numerical verification of the coupled procedures, validated FE-Models of the generic delta wing configuration which comprises the flexible delta wing mounted on the flexible wind tunnel support are available [11] [15]. These models have been developed based on results of both ground vibration and static deformation tests.

3.3.1 Modal Approach

The approach described here is characterized by the use of the multibody system SIMPACK [12] to account for the elastic structure as well as the flight mechanics and its loose coupling to the computational fluid dynamics software TAU. It is called modal approach since the structural elasticity is introduced from a modal solution of the discrete FE-Model, thus receiving a linearly approximated and reduced elastic model which is based on a small number of modal degrees of freedom only. A reasonable number of structural modes have to be chosen to represent the appropriate dynamic behavior. The generic co-simulation interface of the multibody system (MBS) is used for the data exchange to the non-standard CFD partner code which provides the time-accurate aerodynamic solution. The exchanged data is spatially interpolated with the mesh coupling software MpCCI [8] and transferred through a TCP/IP socket.

The features of the modal approach comprising the topics of time and spatial coupling, structural and flight mechanical models are the following:

- Loose coupling for constant communication interval with master (CFD-TAU) and slave (MBS Simpack) process; the underlying time coupling scheme is the "Conventional Serial Staggered" (CSS) algorithm [7].

- MBS time integration method is an implicit BDF2 algorithm (SODASRT, DASSL based).

- Use of conservative and non-conservative, element based interpolation algorithms to map the aerodynamic forces and the deformed mesh coordinates, respectively (MpCCI library).

NATO/PFP UNCLASSIFIED

**Prediction of the Unsteady Behavior of Maneuvering Aircraft by
CFD Aerodynamic, Flight-Mechanic and Aeroelastic Coupling**

- Description of structural elasticity with a reduced, modal approximation computed from the FE-Model.

- Consideration of all translation and rotation degrees of freedom in terms of flight mechanics from the MBS functionality.

The computation of the aerodynamic loads in TAU initiates the coupled computation and acts as master of the co-simulation (loose coupling). SIMPACK delivers the deformed coordinates of the coupling surface as slave. The deformed coordinates are interpolated by MpCCI, and then propagated by the TAU deformation tool into a deformed CFD mesh which is pre-processed for the CFD solver. A more comprehensive description of the simulation platform developed in the modal approach is given in [1].

3.3.2 Discrete Approach

The second aeroelastic method is the so called discrete approach. The underlying spatial coupling scheme is conservative with regards to the forces, moments and the work performed on both the aerodynamic and structure dynamic side. Furthermore, it is verified that no dissipation or accumulation of net energy occurs. This means that at each time-step the sum of kinetic and potential energy of the structure mechanical model and the performed work of the forces on the aerodynamic surface are in equilibrium.

The main characteristics of this fluid structure interaction in the time domain are as follows:

- loose coupling of computational fluid dynamics (CFD) and computational structure dynamics (CSD) through netcdf file input/output,

- time coupling scheme based on adjusted "Conventional Serial Staggered" (CSS) [6] algorithm modified with a predictor-corrector scheme,

- use of an implicit or explicit Newmark algorithm for the time integration of the CSD equations of motion [16],

- use of different scattered data interpolation methods with and without compact support radius for coupling in space domain [2],

- description of the structure mechanic behavior by the reduced, discrete FE-Model of the delta-wing and the support.

Within this approach for the numerical integration of the structure mechanics equations of motion with the Newmark algorithm, reduced system matrices M_{AA} and K_{AA} from a NASTRAN eigenvalue solution are used and updated in each time-step to represent the position change of the delta wing during the flight maneuver. Inside of these matrices only the translatory degrees of freedom that are involved in the spatial coupling algorithm are included. One advantage of this approach is, that all modes of the reduced finite elements structure model and their dependency of each other are considered in the coupling between the different discretized aerodynamic and structure mechanics models.

The software package for this approach is called COUPLING and developed at the DLR Institute of Aeroelasticity. It consists of different subroutines and is written in the MATLAB language. The tool can also be used independently from MATLAB if it has been compiled with the appropriate MATLAB compiler in the C or C++ language [6].

3.4 Integration Framework

For providing an applicable engineering tool it is necessary to have an integration framework organizing the communication between the applications, the management of the simulation scenarios, the data transfer and the capability to distribute the simulation on different computational platforms adapted for the

different numerical codes.

The integration framework TENT [17] provides a graphical user interface for controlling and monitoring coupled simulation workflows. The various codes used in the SikMa simulations will be made available in the TENT system, where a simulation workflow can be built by connecting icons representing each code using a graphical workflow editor. Java wrappers containing the basic control functionality for the TAU and SIMULA applications are already integrated in the TENT environment. The wrapper for the CSM-Code as well as the extension of the functionality to handle the coupling between all three disciplines is under development.

While TENT is providing the data transfer, the communication between the applications and the distribution of the applications on different computational platforms, the communication logic for the simulation workflow is contained within a coupling manager script. The coupling manager is a user-extensible script based on a Python and Java interface, where functionality to control the flow of the simulation has been implemented. In **Fig 1** the graphical user interface of TENT is shown as well the pre-processing tool SimBrowser. The SimBrowser provides the capability to setup the model hierarchy, to define the motion of each element (e.g. flaps, ruder…) and is delivering the necessary motion- and hierarchy-input files for the flow solver.

4. EXPERIMENTAL DATA

For the validation of the numerical simulation software, various wind-tunnel experiments, designed specifically for the SikMa project, are performed. Experimental data, both steady and unsteady, are available for a 65°-swept delta-wing-fuselage-configuration which has been tested in the DNW Transonic-Wind-Tunnel Göttingen (DNW-TWG). The model has movable trailing-edge flaps and can be used for both guided and free-to-roll maneuver simulations around its longitudinal axis. The model shown in **Fig. 2** has a chord length of 482mm and a span of 382mm. For the verification of the aerodynamic-structure coupling a static and dynamic system identification of the delta-wing and the support within the wind tunnel is done. The system parameters are used to set up the FE-Model for the coupled simulation.

The main experiments for the SikMa project are done in the DNW Low-Speed-Wind-Tunnel Braunschweig (DNW-NWB). In order to perform these experiments, a wind-tunnel model has been designed and built for the SikMa project. The model, shown in **Fig. 3**, is based on the X-31 experimental high angle-of-attack aircraft configuration. The model is equipped with remote controlled moveable control devices driven by internal servo-engines, as seen in **Fig. 4**. Measurement equipment is installed to determine the aerodynamic forces and moments on the model, as well as span-wise pressure distributions at locations of 60% and 70% chord length. The experiments include steady-state measurements using PSP-"Pressure Sensitive Paint", which provide detailed information on the surface pressure distribution for the whole wing. The experiments will culminate with maneuver simulations, where the movement of the aircraft and the control devices will be synchronized. For the maneuver experiments the model will be mounted on the MPM-"Model Positioning Mechanism" of the DNW-NWB. **Fig. 5** shows the X-31-Remote-Control model mounted on the MPM-System.

5. RESULTS

For the verification and validation of the simulation environment, the results of the numerical simulations are compared against data collected from various experimental simulations. To show the capability of the TAU-Code to predict the unsteady aerodynamic behavior of configurations with vortex dominated flow fields the delta-wing-configuration described in section 4 is used.

In **Fig. 6** the result of a coupled simulation between CFD and flight-mechanics is shown using the delta-

NATO/PFP UNCLASSIFIED

**Prediction of the Unsteady Behavior of Maneuvering Aircraft by
CFD Aerodynamic, Flight-Mechanic and Aeroelastic Coupling**

wing with trailing-edge flaps. To simulate the motion of the control surfaces (trailing-edge flaps) the chimera approach has been used. The maneuver shown in Fig. 6 is a 1 DoF rotation around the longitudinal axis of the delta-wing induced by an asymmetric deflection of the flaps by $\eta = \pm 3°$. The initial aircraft attitude is at $\alpha = 9°$ and $\Phi = 0°$. The dashed line represents the calculation without any mechanical friction. The solid line represents the calculation supposing a constant dynamic friction. It is seen that the wing tends to go into a periodic roll motion in both the numerical and experimental simulations. It is also seen that the determination of the initial conditions are not correct and the static friction leads in the calculation to a different aerodynamic behavior at the beginning of the simulation. Beside the incorrect determination of the static friction, only a one equation turbulence model is used in this coupled simulation. It is known that for sharp leading-edge delta-wings the k-ω turbulence model delivers better results and will be used in further simulations.

In **Fig. 7** a CFD - flight-mechanics coupled simulation of the delta-wing with trailing edge flaps is depicted. The initial attitudes are now $\alpha = 17°$ and $\Phi_0 = 0°$. The trailing-edge flaps are deflected by $\eta = \pm 5°$ once the model has been released. The turbulence model used for this simulation is the k-ω-model with the Kok-TNT-rotational correction approach [4]. Two calculations are done using this configuration. The first calculation is done without taking into account the effects of mechanical friction, while for the second calculation a mechanical friction of 3.5Nm, which is approximately determined from the experimental data, is implemented. The characteristic movement of the model, as well as the roll-moment coefficient, are well predicted by the second calculation. By analyzing the roll-moment coefficient we observe the following:

- An asymmetric surface force-distribution develops due to the asymmetric trailing-edge flap deflection, which in turn leads to a rotational acceleration around the longitudinal axis of the model.

- The maximum roll-moment coefficient is reached after a simulation time of 0.05s, where the flaps are at $\eta = 2.5°$ deflection. After this the roll-moment coefficient decreases and reaches a temporary plateau at t = 0.1s, at which time the flaps are fully deflected at $\eta = 5°$.

- The model reaches a trim-point at $\Phi = 31°$, where the combined roll-moment is not large enough to overcome the mechanical friction.

The reason for the movement of the model is graphically explained in **Fig. 8**. At the start of the simulation the wing is accelerated due to the asymmetric flap deflection, see Fig. 8.1. The vortex on the luff side of the wing is strengthened with the increasing roll angle. The effective sweep angle on the luff side of the wing is decreasing, which in turn increases the normal component of the on-flow vector. This causes a stronger primary vortex on the luff side, which is located closer to the surface, thus leading to a higher local lift on the luff side. On the lee side the opposite effect happens. The wing vortex gets weaker and the distance from the wing surface higher as the roll angle increases, which leads to a lower local lift on the lee side, see Fig. 8.2. This effect causes the wing to decelerate, which in turn leads to the trim-point at $\Phi = 31°$, Fig. 8.3 and 8.4.

Both examples show the capability of CFD-flight-mechanics coupling by means of a delta-wing with trailing edge flaps. The main aerodynamic effects are qualitatively well predicted, but in order to predict the quantitative aerodynamic values obtained experimentally it is necessary to have the same starting conditions and environment parameters that were in effect during the experimental maneuver scenario. If the starting conditions are not the same, the prediction of the experimentally obtained final condition can not be guaranteed.

The capability to predict the elastic deformations of the delta-wing configuration during a guided roll

maneuver should be demonstrated as follows. In the coupled simulation between the TAU-Code and the structural mechanics tool developed within the discrete approach, the delta-wing and the rear-sting support are considered to be elastically deformable. For the coupled simulation, the FE-model [15] takes into account both the delta wing configuration as well as the flexible support, as seen in **Fig. 9**. The FE-Model is validated based on results of both ground vibration and static deformation tests. The aerodynamic simulations base on Euler calculations using a coarse mesh topology to reduce the unsteady calculation time on the CFD side. For the verification of the capabilities this procedure is sufficient.

In **Fig. 10** the corresponding history of the model deflection due to the elasticity is seen. Depicted is the displacement of the sting support at the trailing-edge of the delta wing. It is seen that the sting is describing an elliptic motion during the rotation. The green loop in **Fig. 10** shows the sting movement from the experiment due to the integration of the measured accelerations. Because of the integration the shift in z-direction can not be captured. However, it is shown that the numerical simulations predict the characteristic movement of the sting accurately. Due to this deformation the effective angle-of-attack of the delta wing at the same roll angle is higher in the elastic case than for the rigid body motion. This leads to higher amplitudes of the rolling moment, as is seen in **Fig. 11**.

The time-history results of the rigid and the coupled elastic simulation of the free-to-roll wind tunnel maneuver are compared in **Fig. 12** for the roll angle Φ and in **Fig. 13** for the rolling moment L, respectively. The on flow mach number is at $Ma = 0.5$, the angle-of-attack is at 9° and the initial roll angle is at $\Phi_0 = 45°$. As described before, the maneuver is initiated by the unsymmetrical load distribution over wing surface due to the initial roll angle. Furthermore, the same effects occur as in the guided maneuver simulation. The deformations of the model in y- and z-direction lead to locally higher angles of attack and thus to higher rolling moments, as seen in Fig. 12. In comparison to the rigid body motion in case of the discrete approach the maneuver shows a higher damping, as seen in Fig. 13. The same effect is expected for the modal approach but in this case the CFD solution is not sufficiently converged to get the same effects. However, the capability and necessity is shown to consider the structural behavior in maneuver simulations.

For the X-31 configuration, results from steady-state numerical simulations have been obtained. These simulations show the capability of the TAU-Code to simulate complex delta-wing configurations with rounded leading-edges. **Fig. 14** shows the numerically simulated 3D flow field over the X-31 configuration, which is a good indication of the complexity of the vortex flow topology over the wing and fuselage. Comparisons with experimental data show good agreement regarding the vortex topology. In **Fig. 15a** an oil flow picture of the X-31 clean-wing from low speed experiments is shown. The angle-of-attack is $\alpha = 18°$ at a Reynolds number of 1.0Mio. The attachment line of the strake vortex and the main wing vortex as well as the separation line of the main wing vortex near the leading-edge is emphasized. In **Fig. 15b** the corresponding CFD calculation is depicted. It is seen that the flow topology from the calculation fits quite well with the experiment. Further experimental results delivering steady pressure distributions upon the wing were done within another X-31 test campaign. The PSP result at $\alpha = 18°$ at a Reynolds number of 2.07Mio is shown in **Fig. 16a**. Comparing the pressure distribution from the PSP measurement with the CFD calculation in **Fig. 16b** it is seen that the main footprints of the vortices are captured by the numeric, but not accurately the suction-strength and the vortex location. Further investigations will be done for this complex fighter aircraft configuration to capture the correct aerodynamics by CFD calculations.

NATO/PFP UNCLASSIFIED

Prediction of the Unsteady Behavior of Maneuvering Aircraft by CFD Aerodynamic, Flight-Mechanic and Aeroelastic Coupling

6. CONCLUSIONS

In this paper the activities and recent results of the DLR-Project SikMa were presented. In SikMa a simulation tool will be developed that is capable of simulating a maneuvering elastic aircraft with all its moveable control devices. The simulation tool combines time-accurate aerodynamic, aeroelastic and flight-mechanic calculations to achieve this objective. Preliminary verification of the functionality of the simulation tool has been shown by simulating a sharp leading-edge delta-wing during free-to-roll maneuvers due to flap deflections. Furthermore, first perspectives were presented regarding the time-accurate coupling between the TAU-Code and the numerical Structure Mechanical Tool. Initial results of the steady flow field around the X-31 configuration were presented. The next steps in the SikMa project will be amongst others a coupled simulation of CFD and CSM using a RANS model on the CFD side instead of the Euler simulation and the unsteady maneuver simulation of the X-31 by simulating all control devices. Finally an engineering tool for the simulation of flight maneuvers using high performance numerical tools will be available.

7. REFERENCES

[1]   Arnold, J.; Einarsson, G.; Gerhold, T.: Time-Accurate Simulation of a Maneuvering Aeroelastic Delta Wing at High Angle-of-Attack. Proc ICAS 2004, Yokohama, Japan; 2004.

[2]   Beckert, A.; Wendland, H.: Multivariate Interpolation for Fluid-Structure-Interaction Problems using Radial Basis Functions. Aerospace Science and Technology, Art. No. 5125, 2001.

[3]   Centaur Soft: http://www.Centaursoft.com

[4]   Dol, H.S.; Kok, J.C.; Oskam, B.: Turbulence modeling for leading-edge vortex flows. AIAA 2002-0843, Reno, Jan. 2002.

[5]   Dwight, R.P.: Time-Accurate Navier-Stokes Calculations with Approximately Factored Implicit Schemes. Proceedings of the ICCFD3 Conference Toronto, Springer, 2004.

[6]   Einarsson, G.; Neumann, J.: Multidisciplinary Simulation of a Generic Delta Wing: Aerodynamic, Flight-Dynamic, and Structure-Mechanic Coupling. ECCOMAS, International Conference on Computational Methods for Coupled Problems in Science and Engineering, Santorini Island, 2005.

[7]   Farhat C.; Lesoinne M.: Higher-Order Staggered and Subiteration Free Algorithms for Coupled Dynamic Aeroelasticity Problems. AIAA 98-0516, 1998.

[8]   Fraunhofer Institute for Algorithms and Scientific Computation SCAI: MpCCI Mesh based parallel code coupling interface. Specification of MpCCI version 2.0, 2003.

[9]   Galle, M.; Gerhold, T.; Evans, J.: Technical Documentation of the DLR TAU-Code DLR-IB 233-97/A43 1997

[10] Gerhold, T.; Galle, M.; Friedrich, O.; Evans, J.: Calculation of Complex Three-Dimensional Configurations employing the DLR TAU-Code. AIAA-97-0167 1997.

[11] Hoffmann, D.; Neumann, J.; Sinapius, M.: Strukturmechanische Identifikation von Halterung und Windkanalmodell "AeroSUM". DLR-IB, IB 232-2002-C06, 2002.

[12] Lugner, P.; Arnold, M.; Vaculin, O. (Eds): Vehicle System Dynamics (Special issue in memory of Professor Willi Kortüm). Vol. 41, No. 5, 2004.

[13] Madrane, A.; Raichle, A.; Stürmer, A.: Parallel implementation of a dynamic overset unstructured grid approach. ECCOMAS Conference Jyväskylä Finland, 24.-28. July 2004.

[14] Mönnich, W.; Buchholz, J. J.: SIMULA - Ein Programmpaket für die Simulation dynamischer Systeme - Dokumentation und Benutzeranleitung - Version 2 DFVLR Institutsbericht IB 111-91/28, 1991.

[15] Neumann, J.: Strukturmechanische und strukturdynamische Finite Element Modelle des Windkanalmodells "AeroSUM" mit Halterung. DLR-IB, IB 232-2003-J01, 2003.

[16] Schulze, S.: Numerische Integration der aeroelastischen Bewegungsgleichungen eines Flügelprofils. DLR-IB, IB 232-94 J 06, 1994.

[17] Schreiber, A.: The Integrated Simulation Environment TENT. Concurrency and Computation:

NATO/PFP UNCLASSIFIED

**Prediction of the Unsteady Behavior of Maneuvering Aircraft by
CFD Aerodynamic, Flight-Mechanic and Aeroelastic Coupling**

Practice and Experience, Volume 14, Issue 13-15, S.1553-1568, 2002.

[18] Schütte, A.; Einarsson, G.; Schöning, B.; Madrane, A.; Mönnich, W., Krüger, W.: Numerical simulation of manoeuvring aircraft by aerodynamic and flight mechanic coupling. RTO AVT-Symposium Paris, 22.-25. April 2002.

[19] Schütte, A.; Einarsson, G.; Schöning, B.; Raichle, A.; Mönnich, W.; Neumann, J.; Arnold, J; Heinecke, J.: Numerical simulation of maneuvering combat aircraft. AG-STAB, STAB-Symposium, Nov.2004, Bremen.

NATO/PFP UNCLASSIFIED

Prediction of the Unsteady Behavior of Maneuvering Aircraft by CFD Aerodynamic, Flight-Mechanic and Aeroelastic Coupling
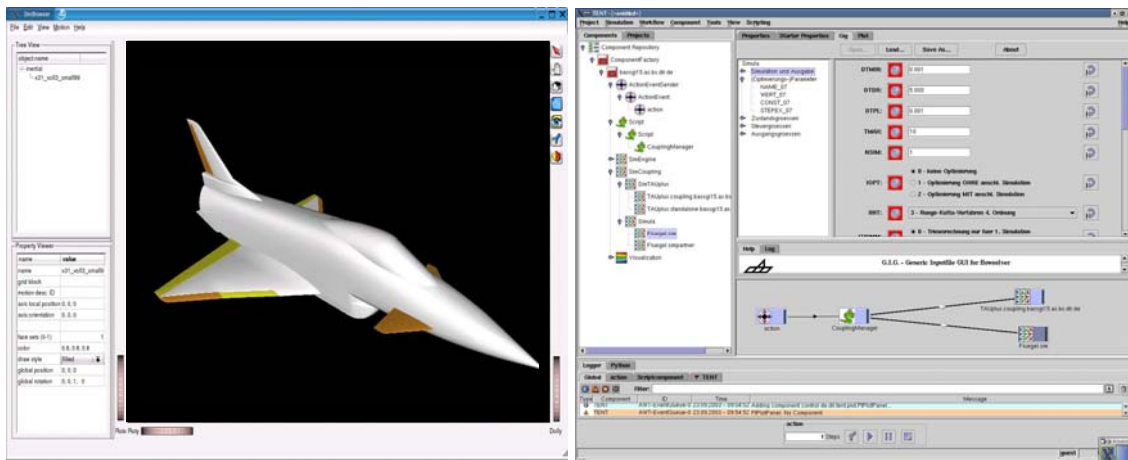
8. FIGURES

Figure 1: Graphical user interface of TENT framework environment and pre-processing tool SimBrowser.

Figure 2: 65°-swept delta-wing-fuselage-model-configuration with remote controlled trailing-edge flaps on the roll-rig device in the DNW-TWG Göttingen.

NATO/PFP UNCLASSIFIED

**Prediction of the Unsteady Behavior of Maneuvering Aircraft by
CFD Aerodynamic, Flight-Mechanic and Aeroelastic Coupling**

Figure 3: X-31 Remote control model in the DNW-NWB Braunschweig.
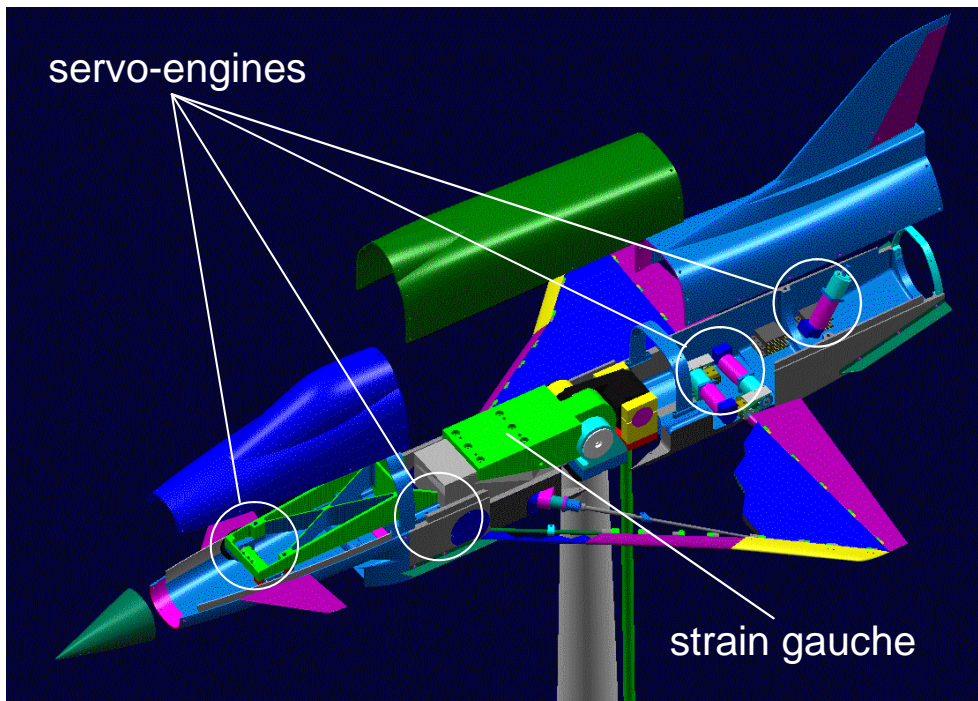
Figure 4: CATIA image of the X-31 wind tunnel model.

NATO/PFP UNCLASSIFIED

**Prediction of the Unsteady Behavior of Maneuvering Aircraft by
CFD Aerodynamic, Flight-Mechanic and Aeroelastic Coupling**

Figure 5: X-31 model on the Model-Positioning-Mechanism in the DNW-NWB wind tunnel.
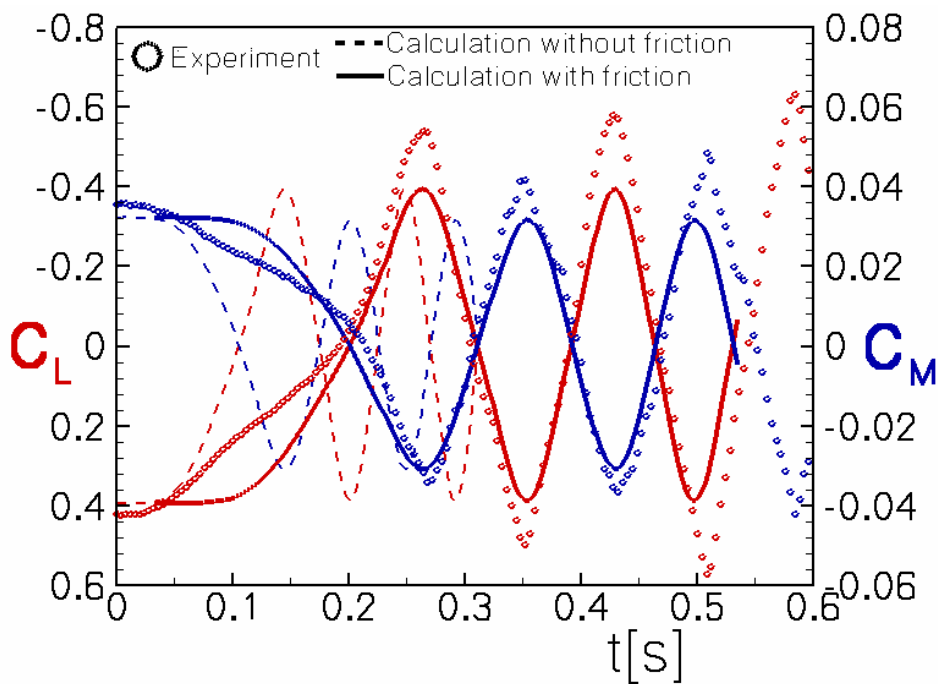
Figure 6: 1 DoF Free-to-Roll maneuver of delta-wing-flap conf. through trailing-edge flap deflection. Ma = 0.85, Re = 5Mio., $\Theta = 9°$, $\Phi_0 = 0°$, $\eta = \pm 3°$.
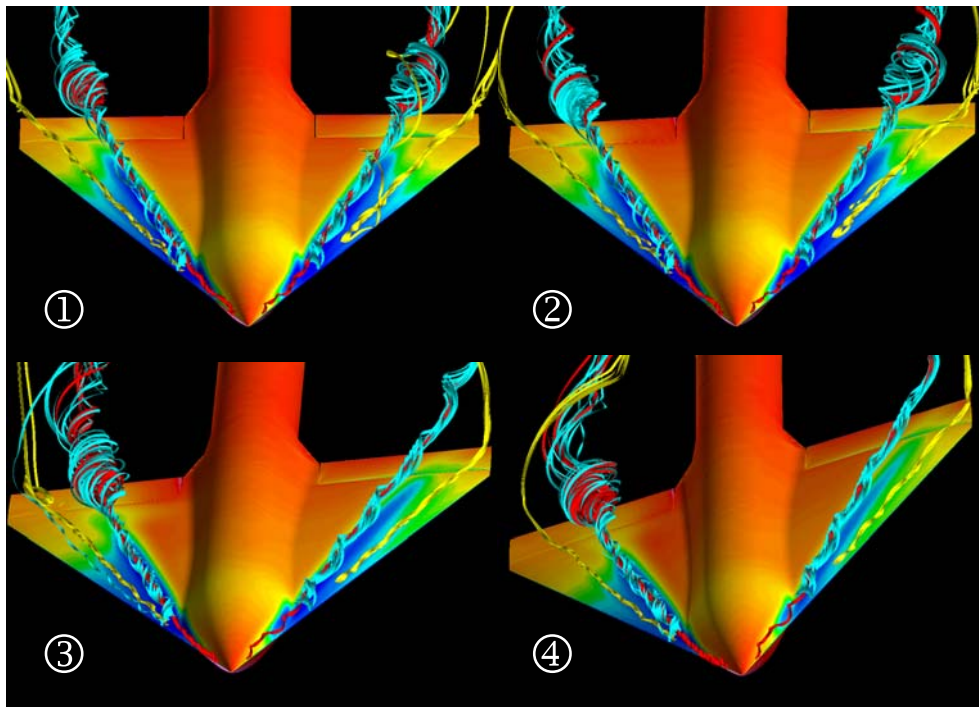
NATO/PFP UNCLASSIFIED

**Prediction of the Unsteady Behavior of Maneuvering Aircraft by
CFD Aerodynamic, Flight-Mechanic and Aeroelastic Coupling**
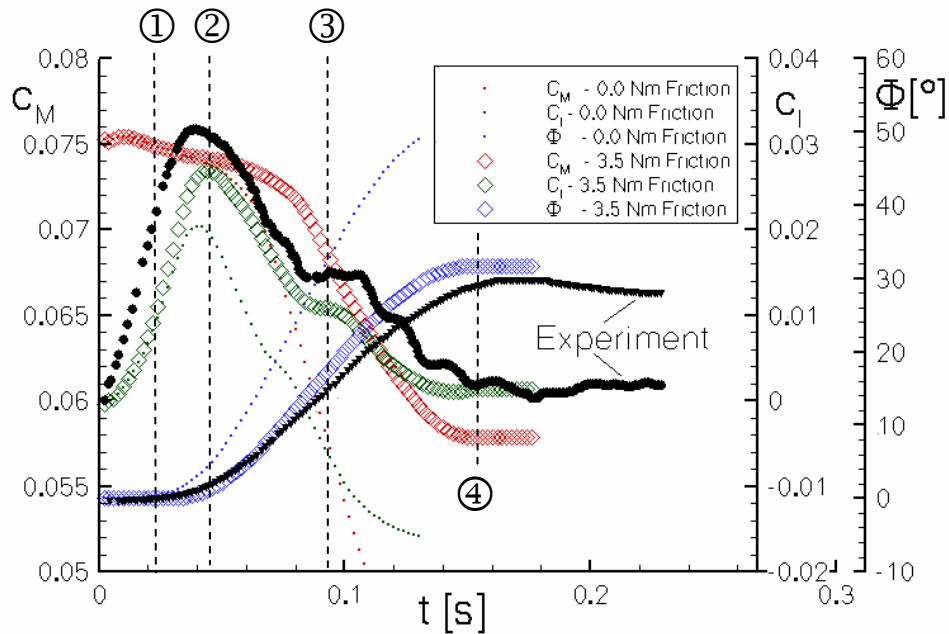
**Figure 7: 1 DoF Free-to-Roll maneuver of delta-wing-flap conf. through trailing-edge
flap deflection. Ma = 0.5, Re = 3.8Mio., $\Theta = 17°$, $\Phi_0 = 0°$, $\eta = \pm 5°$.**

**Figure 8: 1 DoF Free-to-Roll maneuver of delta-wing-flap conf. through trailing-edge
flap deflection. Flow topology at four different stages.
Ma = 0.5, Re = 3.8Mio., $\Theta = 17°$, $\Phi_0 = 0°$, $\eta = \pm 5°$.**

NATO/PFP UNCLASSIFIED

**Prediction of the Unsteady Behavior of Maneuvering Aircraft by
CFD Aerodynamic, Flight-Mechanic and Aeroelastic Coupling**
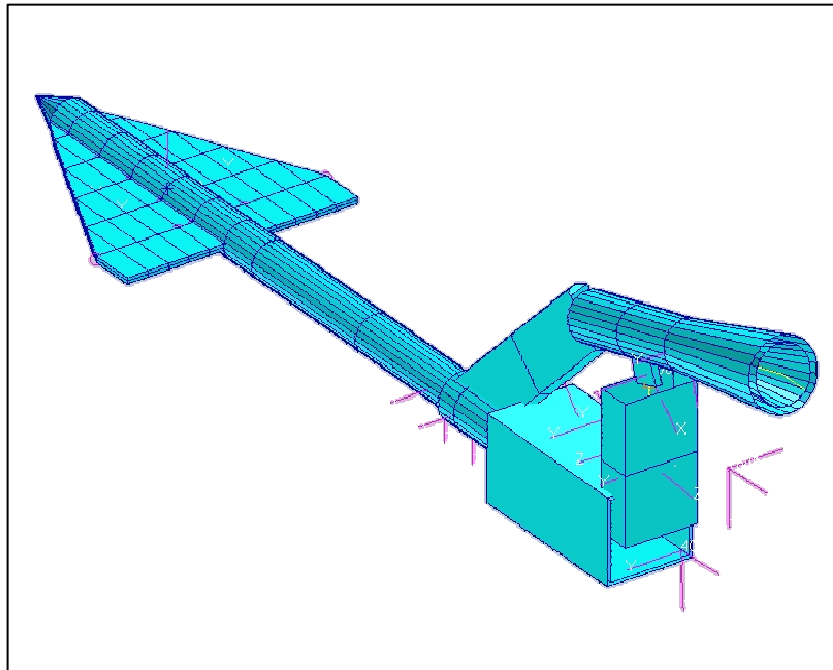
Figure 9: FE-Model of the wind tunnel setup comprising the generic
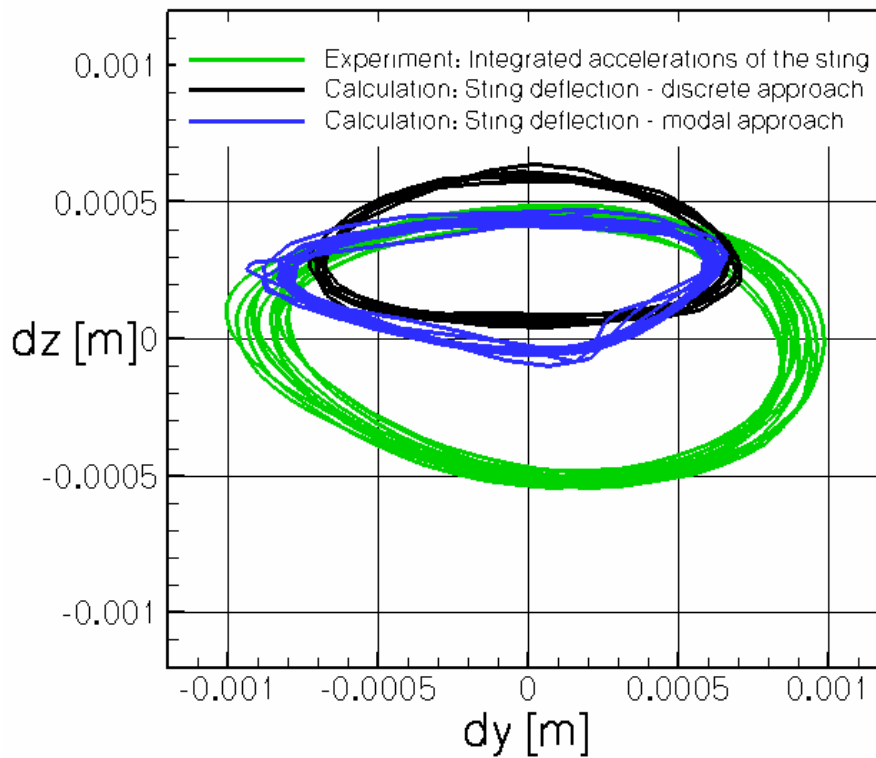delta wing and the model sting.

Figure 10: History of the delta-wing sting deflection during elastic-body motion
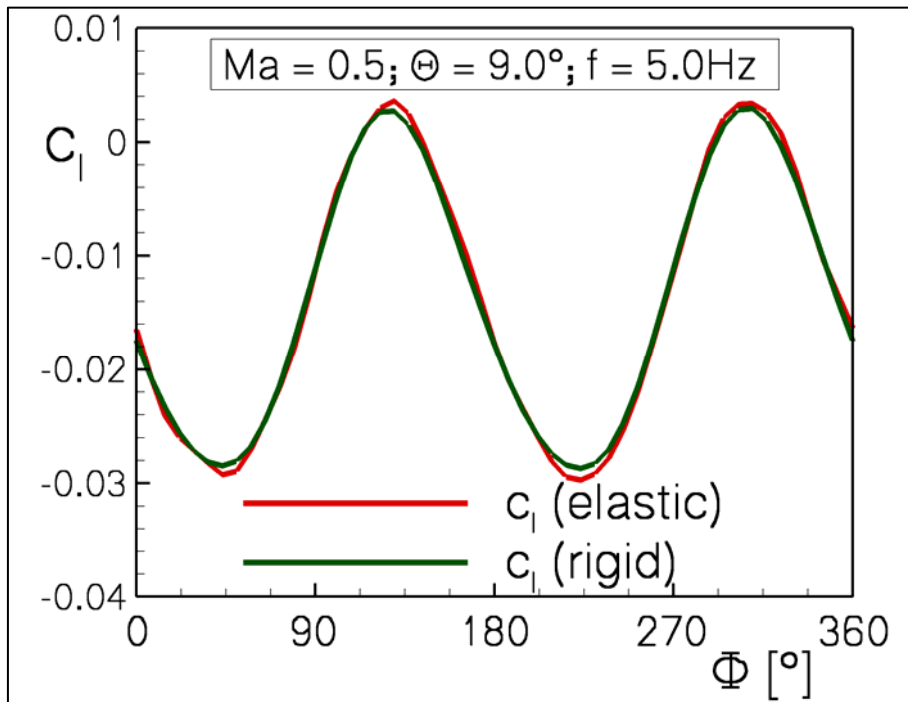comparison with experiment. Time-accurate coupled CFD(Euler)-CSM
simulation

NATO/PFP UNCLASSIFIED

**Prediction of the Unsteady Behavior of Maneuvering Aircraft by
CFD Aerodynamic, Flight-Mechanic and Aeroelastic Coupling**

Figure 11: Comparison of rolling moment between rigid- and elastic-body motion of
delta-wing during constant rotational movement. Time-accurate coupled
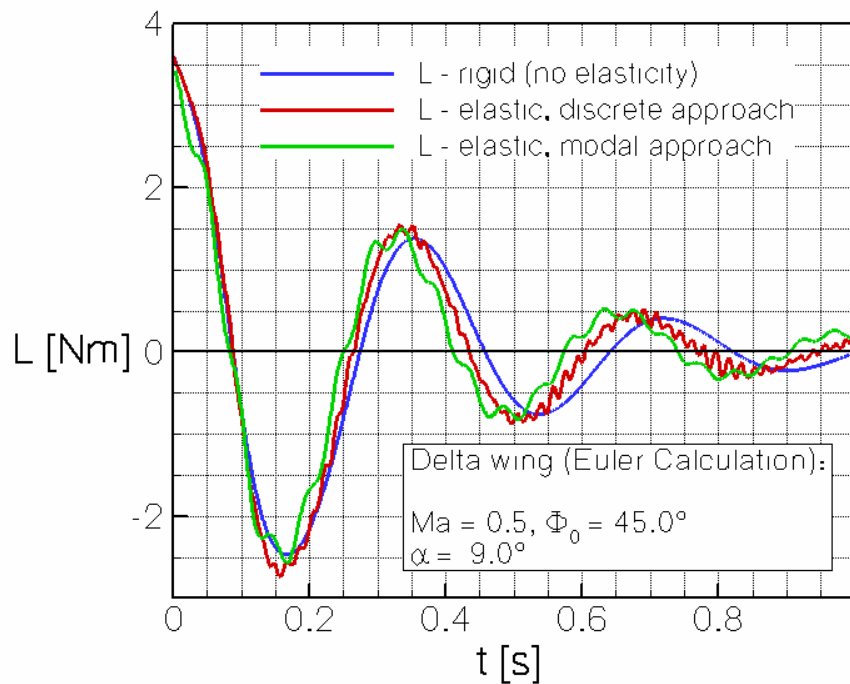CFD(Euler)-CSM simulation.

Figure 12: Comparison of the aerodynamic moment L for a free to roll maneuver for
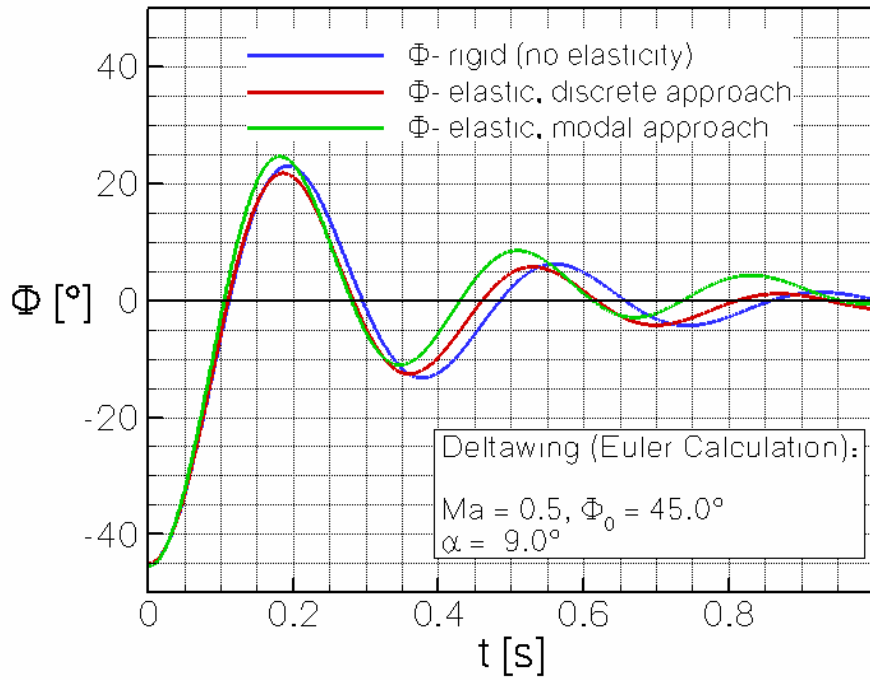rigid motion and elastic motion with different approaches

NATO/PFP UNCLASSIFIED

**Prediction of the Unsteady Behavior of Maneuvering Aircraft by
CFD Aerodynamic, Flight-Mechanic and Aeroelastic Coupling**

Figure 13: **Comparison of the roll angle Φ for a free to roll maneuver for rigid motion
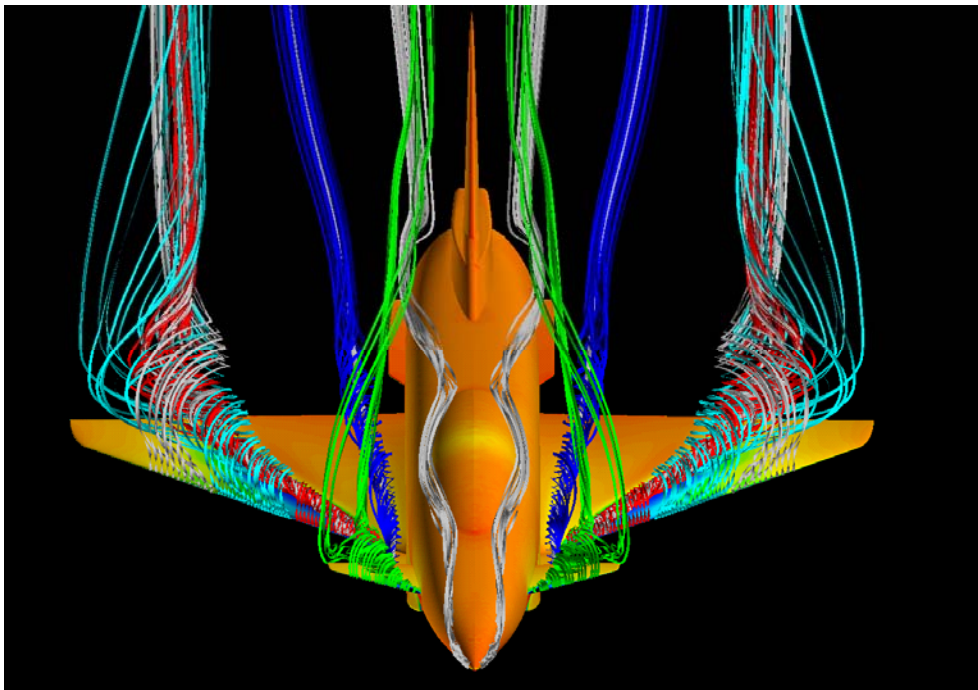and elastic motion with different approaches**

Figure 14: 3D flow field over the X-31 configuration at 18⁰ angle-of-attack.

NATO/PFP UNCLASSIFIED

**Prediction of the Unsteady Behavior of Maneuvering Aircraft by
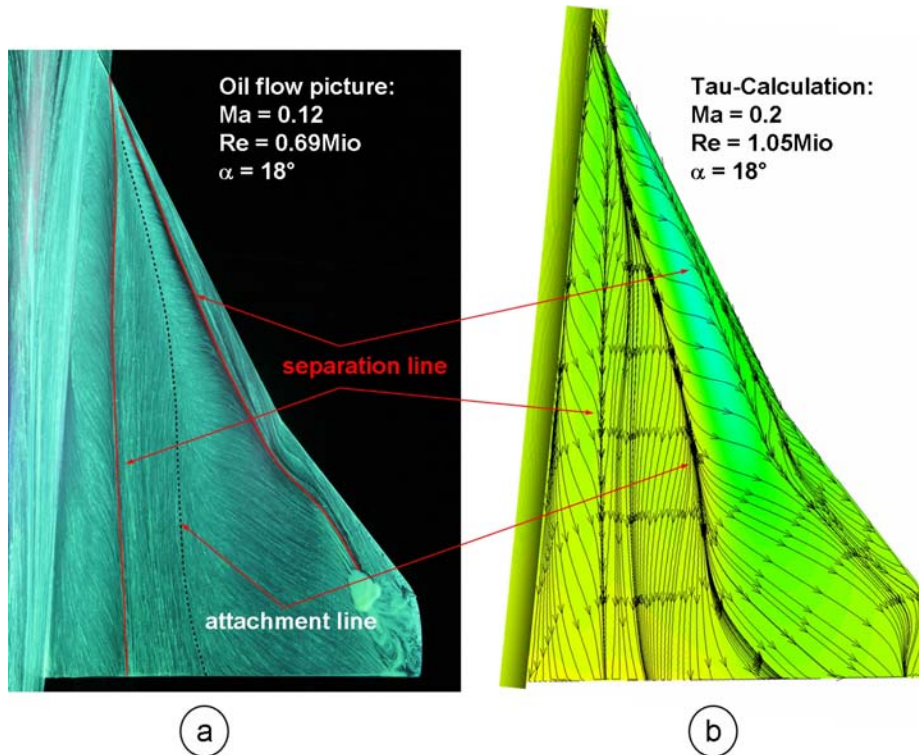CFD Aerodynamic, Flight-Mechanic and Aeroelastic Coupling**

**Figure 15: a) Oil flow visualization of the X-31 clean wing at $\alpha = 18^0$.
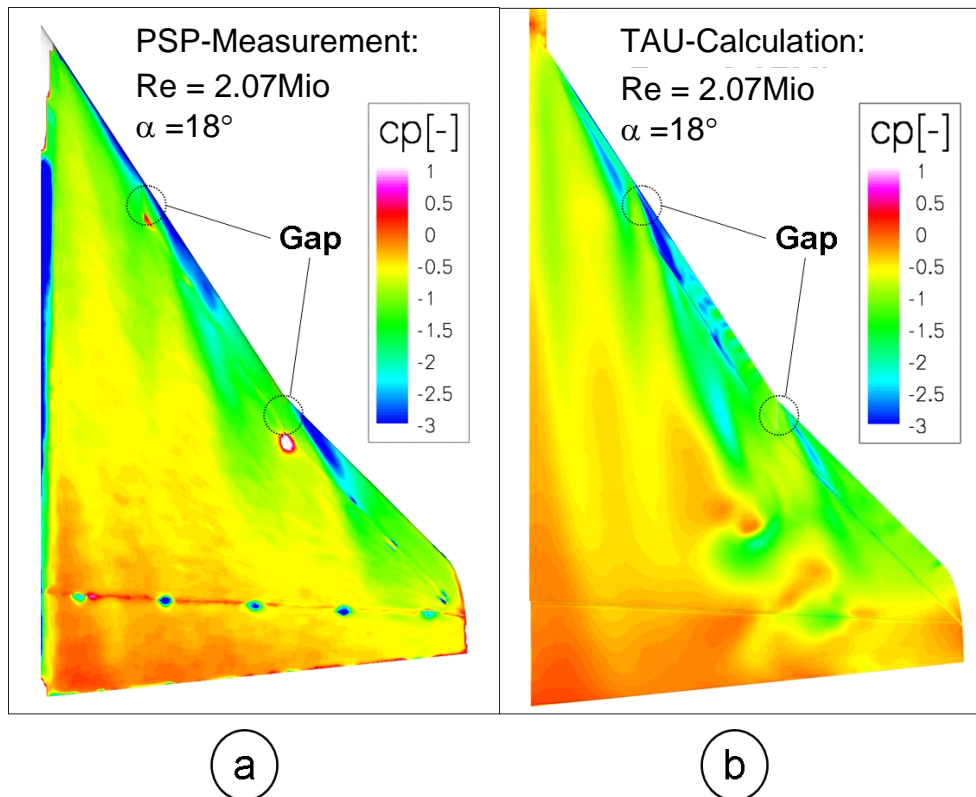b) TAU calculation: Visualization of surface streamlines at $\alpha = 18^0$.**

**Figure 16: a) Steady PSP measurement of the pressure distribution over the X-31 wing.
b) Steady TAU RANS calculation of the pressure distribution over the X-31
wing.**